

# GEOFISICA INTERNACIONAL

REVISTA DE LA UNION GEOFISICA MEXICANA, AUSPICIADA POR EL INSTITUTO DE  
GEOFISICA DE LA UNIVERSIDAD NACIONAL AUTONOMA DE MEXICO

Vol. 25

México, D. F., 1o. de abril de 1986

Núm.2

## *SYNTHETIC SEISMOGRAMS FOR A DISLOCATION SOURCE BY FINITE-DIFFERENCE TECHNIQUES*

J. M. ESPINDOLA-CASTRO\*

L. W. BRAÏLE\*\*

*(Received: October 19, 1984)*

*(Accepted: December 10, 1985)*

### ABSTRACT

A method to compute synthetic seismograms from a dislocation source in heterogeneous media by finite-difference techniques is presented. The model consists of a two-dimensional region in skew coordinates. With this technique it is possible to take into account the free surface and different geometric and kinematic characteristics of the source.

### RESUMEN

Se presenta un método para calcular sismogramas sintéticos de una dislocación en dos dimensiones. El método utiliza diferencias finitas en coordenadas no ortogonales. Con esta técnica es posible modelar medios heterogéneos con superficie libre y dislocaciones con diferentes características geométricas y cinemáticas.

\* Instituto de Geofísica, UNAM, C. U., México, D. F., MEXICO.

\*\* Department of Geosciences, Purdue University, West Lafayette, Ind. 47907, U. S. A.

## INTRODUCTION

The gross features of the seismic source have been successfully modeled by means of kinematic models. Although several limitations are inherent to the theory (Brune, 1970, Anderson and Richards, 1975; Madariaga, 1978) it still provides a useful tool in earthquake research. In this paper we give solutions to the in-plane dislocation problem by means of an explicit finite-difference (F-D) technique in skew-coordinates.

The (F-D) method allows consideration of vertical and lateral heterogeneities and supplies great flexibility in the choice of fault parameters.

## THE FINITE DIFFERENCE SOLUTION

The model to be considered here is the in-plane two dimensional case. The elastic equations of motion in this instance are:

$$\rho \frac{\partial^2 u}{\partial t^2} = \frac{\partial}{\partial x} \left( \lambda \left( \frac{\partial u}{\partial x} + \frac{\partial w}{\partial z} \right) + 2\mu \frac{\partial u}{\partial x} \right) + \frac{\partial}{\partial z} \left( \mu \left( \frac{\partial w}{\partial x} + \frac{\partial u}{\partial z} \right) \right) \quad (1)$$

$$\rho \frac{\partial^2 w}{\partial t^2} = \frac{\partial}{\partial z} \left( \lambda \left( \frac{\partial u}{\partial x} + \frac{\partial w}{\partial z} \right) + 2\mu \frac{\partial w}{\partial z} \right) + \frac{\partial}{\partial x} \left( \mu \left( \frac{\partial w}{\partial x} + \frac{\partial u}{\partial z} \right) \right)$$

where  $u$  and  $w$  are the horizontal and vertical displacements,  $\rho$  is the density,  $t$  is time and  $\lambda$  and  $\mu$  are Lamé's constants of the medium.

The condition of vanishing of stress at the free surface requires that,

$$\frac{\partial w}{\partial x} + \frac{\partial u}{\partial z} = 0$$

$$\frac{\partial w}{\partial z} + \frac{\lambda}{\lambda + 2\mu} \frac{\partial u}{\partial x} = 0 \quad (2)$$

There exists in addition the condition of dislocation,

$$u = u^+ - u^- = D(r, t - V_r/r)$$

Here,  $D(r, t - V_r/r)$  is the relative displacement across the fault  $V_r$  the velocity of rupture and  $r$  the direction in which the fault propagates.

An explicit F.D. scheme may be obtained from the equations by substituting the partial derivatives by F.D. operators. In this process the space as well as time become discrete variables.

In the case of equation (1) its F.D. approximation allows the computation of displacements at time  $t+1$  in terms of displacements at times  $t$  and  $t-1$  as shown in Figure 1. Full expressions of the scheme have been given among others by Kelly *et al.* (1976).

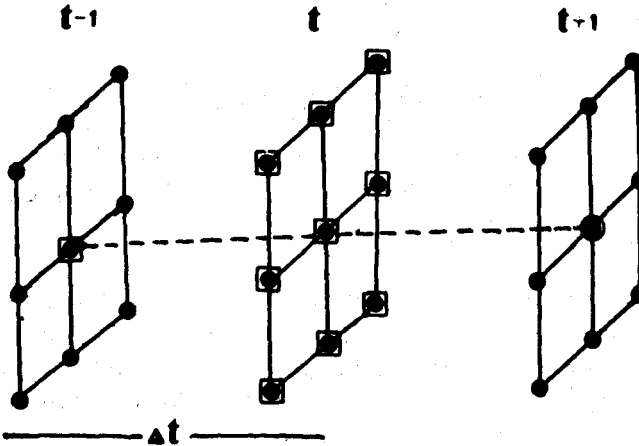


Fig. 1. The computation scheme requires the values of displacement at the points in the squares (times  $t$  and  $t-1$ ) in order to compute the displacements at the encircled dot (time  $t+1$ ).

First and Second order schemes for equation (2) are given by Alterman and Karal (1968) and Ilan *et al.* (1975). The displacements at the free surface may be computed from any of these schemes.

Because of the finite memory of the computer, artificial boundaries must be placed in the region of computation.

These artificial boundaries require the specification of Dirichlet or Neumann conditions so that the computation may be carried out in the whole region but then undesirable reflections arise. Clayton and Engquist (1977) have devised a procedure, based on paraxial approximations to the wave equation, that minimize this problem. Two paraxial approximations are derived by these authors. These are:

$$\frac{\partial U}{\partial z} + B_1 \frac{\partial U}{\partial t} = 0 \tag{a}$$

$$\frac{\partial U}{\partial t \partial z} + C_1 \frac{\partial U}{\partial t^2} + C_2 \frac{\partial U}{\partial t \partial x} + C_3 \frac{\partial U}{\partial x^2} = 0 \tag{b}$$

(4)

where

$$U = \begin{pmatrix} u \\ w \end{pmatrix}; B_1 = C_1 = \begin{pmatrix} 1/\beta & 0 \\ 0 & 1/\alpha \end{pmatrix}; C_2 = (\beta - \alpha) \begin{pmatrix} 0 & 1/\beta \\ 1/\alpha & 0 \end{pmatrix}$$

$$\text{and } C_3 = \frac{1}{2} \begin{pmatrix} \beta - 2\alpha & 0 \\ 0 & \alpha - 2\beta \end{pmatrix}$$

The first of equations (4) is appropriate for points at the corners of the mesh while the second one may be used in the rest of the points on the artificial boundaries. The absorption provided by these equations depends on the angle of incidence of the radiation with 100% absorption for radiation incident perpendicular to the boundary.

The condition of dislocation (equation 3) may be easily applied once the previous schemes have been implemented. To this effect a segment of a column of nodes representing the fault plane is chosen and the points along it given a specified displacement time-history. Points on one side of the fault will take this displacement as positive and points on the opposite side as negative.

The finite velocity of rupture is simulated by merely delaying the onset of displacement between one point and the following. If the delay is of  $n$  time-steps the velocity of rupture is

$$V_r = \frac{h/2}{n\Delta t} \quad (5)$$

where  $h$  is the grid interval and  $\Delta t$  the time-step. The relative displacement at each point that simulates the fault may be prescribed as a function of the time step.

Figure 2(a) shows in a schematic way the manner in which the schemes so far discussed are applied to the region of computation.

From Figure 2(a) it is also evident that faults with dips other than  $90^\circ$  would require for close points to use displacements on both sides of the fault plane. Since the fault should act as a reflector this would yield incorrect results.

One way to avoid this problem is to pose the problem in skew coordinates (Salvadori and Baron, 1961). In these coordinates the derivatives of the rectangular system are transformed according to

$$\frac{d}{dx'} = \frac{d}{dx}$$

$$\frac{d}{dz'} = \frac{1}{\sin \theta} \left( \frac{d}{dz} - \cos \theta \frac{d}{dx} \right) \quad (6)$$

where  $\theta$  is the angle between the coordinate axes taken in the clockwise sense.

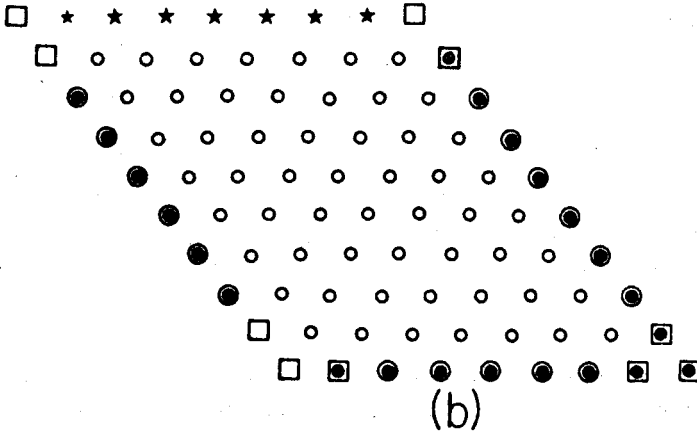
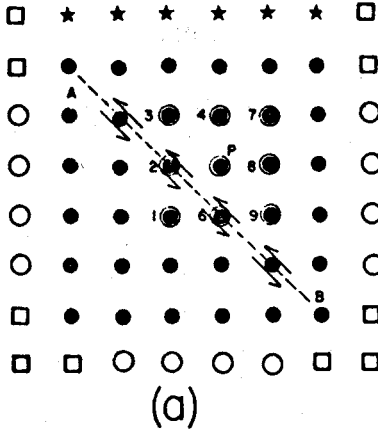


Fig. 2(a) Computational grid. Dots indicate points where the complete wave equation (equation (1)) is used. Stars are computed by means of equations (2). Squares and circles are solved through paraxial approximations 4(a) and (b) respectively. Note that if points A, 2, 6 and B represent a fault, the computation of displacements at P would require the displacement at point 1 on the other side of the fault. (b) Computational grid in skew coordinates.

Transformation of relations 1 to 4 according to this rule yield equations that are treated in the same fashion as those in rectangular coordinates to obtain F.D. approximations that will allow the specification of any fault dip. Full expressions appear in the appendixes. Figure 2(b) shows the computational grid in skew-symmetric coordinates.

### LIMITATIONS

The limitations due to the computational procedures will be discussed here; those due to the model itself have already been referred to in the first paragraph of the introduction.

In the discrete approximation to the wave equation, dispersion of the body waves takes place. Boore (1972) and Kelly *et al.* (1976) have discussed this effect. It has been found that, as a rule of thumb to minimize dispersion ten points per wavelength for the highest frequency present should be taken. In the present case the frequency content of the source will be given by the time-history of displacement of the points along the fault. Thus, one should be aware of the meaning of the different frequencies in the synthetic seismograms.

Another important factor to be taken into account in F.D. calculations is the stability of the solutions. Alterman and Loewenthal (1970) have shown that for the wave equation in homogeneous medium the condition of stability is given by:

$$\Delta t < \frac{h}{\sqrt{\alpha^2 + \beta^2}} \quad (7)$$

where  $\alpha$  and  $\beta$  are the P and S wave velocities.

This condition seems to work for heterogeneous mediums as well (Kelly *et al.*, 1976), nevertheless when skew coordinates are employed this condition no longer holds.

No analysis of stability in skew coordinates was carried out because stability inside the region would not necessarily insure stability at the absorbing boundaries where the paraxial approximations are being used. Nevertheless an estimate may be obtained by writing equation (8) in terms of the diagonal of the square grid,

$$\Delta t < \frac{d}{\sqrt{2\alpha^2 + 2\beta^2}} \quad (8)$$

where  $d$  is the length of the diagonal.

In skew coordinates a parallelogram of side  $h$  has a minor diagonal given by

$$d = 2h \sin(\theta/2) \quad (9)$$

Substitution of (10) in (9) yields

$$\Delta t < \frac{2h \sin(\theta/2)}{\sqrt{2\alpha^2 + 2\beta^2}} \quad (10)$$

This inequality was used as an upper limit in the choice of  $h$  and  $\Delta t$ .

An obvious limitation from this approach is that for very small angles of dip many more points will be required to cover the same region than in the case of a rectangular mesh. Concurrently, the time-step should be lowered in order to preserve stability. Both of these factors will increase the cost of computation but this is not too serious for moderate angles of dip ( $45^\circ$ ).

#### EXAMPLES

Computer solutions of equations (1) require 3 arrays for  $\lambda$ ,  $\mu$  and  $\rho$ . In order to reduce these requirements, in the examples that follow, either  $\rho$  has been taken as a constant and then the constants of the medium are written in terms of  $\alpha$  and  $\beta$  or  $\rho$  has been computed from Birch's relationship (Birch, 1964)

$$\rho = 0.252 + 0.3788 \alpha \quad (11)$$

and  $\lambda$  equal to  $\mu$ . A Fortran IV program based on the equations here presented was made and tested for convergence, consistency and stability. The following examples show the versatility of the F.D. scheme to accommodate different characteristics of fault and medium. A first example compares the F.D. solutions with those of Haskell (1969) and Boore and Zaback (1974) which are well known to seismologists.

For this last case, the geometry and variables are shown in Figure 3.  $P_1$  to  $P_5$  are the points of observation. The time history is a ramp function of constant slip. The mesh consisted of 4 620 grid points with  $h = 0.2$  and  $t = 0.05$ . In the case of Haskell's model, which is three-dimensional the fault is 10 times the width of the fault in length.

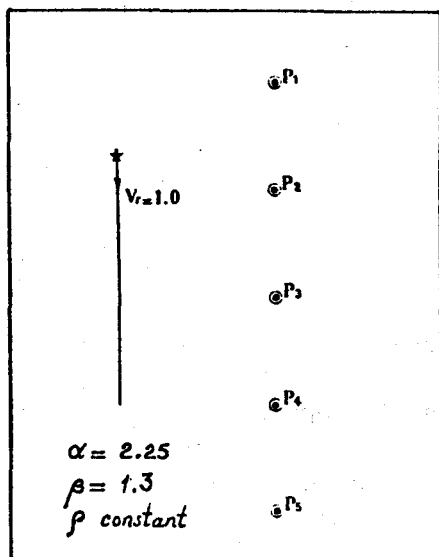


Fig. 3. Geometry of the computational model. The star shows the place where the rupture starts. Points P1 to P5 are sites where the displacements will be displayed. The computational grid has 60 points in the horizontal and 77 in the vertical. Grid spacing is 0.2 km and the time step is .05 sec. The source function is a ramp with the time of 1 sec and constant slip along the fault. Other parameters are shown in the figure.

Figures 4a to 4e show synthetic seismograms at the points of observation. The most pronounced differences are produced by: 1) *Dispersion*. This is conspicuous in the late arrival of high-frequencies. A choice of a time-history other than the ramp-function would have greatly reduced this problem. Figure 5 shows the results of a coarser mesh; the effect of the grid size is readily apparent. 2) *Partial reflections*. This is due to radiation arriving to the boundaries at small angles of incidence. Note that the worst cases are for points close to the artificial boundaries, especially the lower one (P5) since this point is closer to a boundary and farther to the point of initial rupture so that the partial reflections of the artificial boundaries arrive not much later than the signals from the successive points on the fault line. The effects of source parameters and medium on the ground motion at the surface are demonstrated by the following examples.

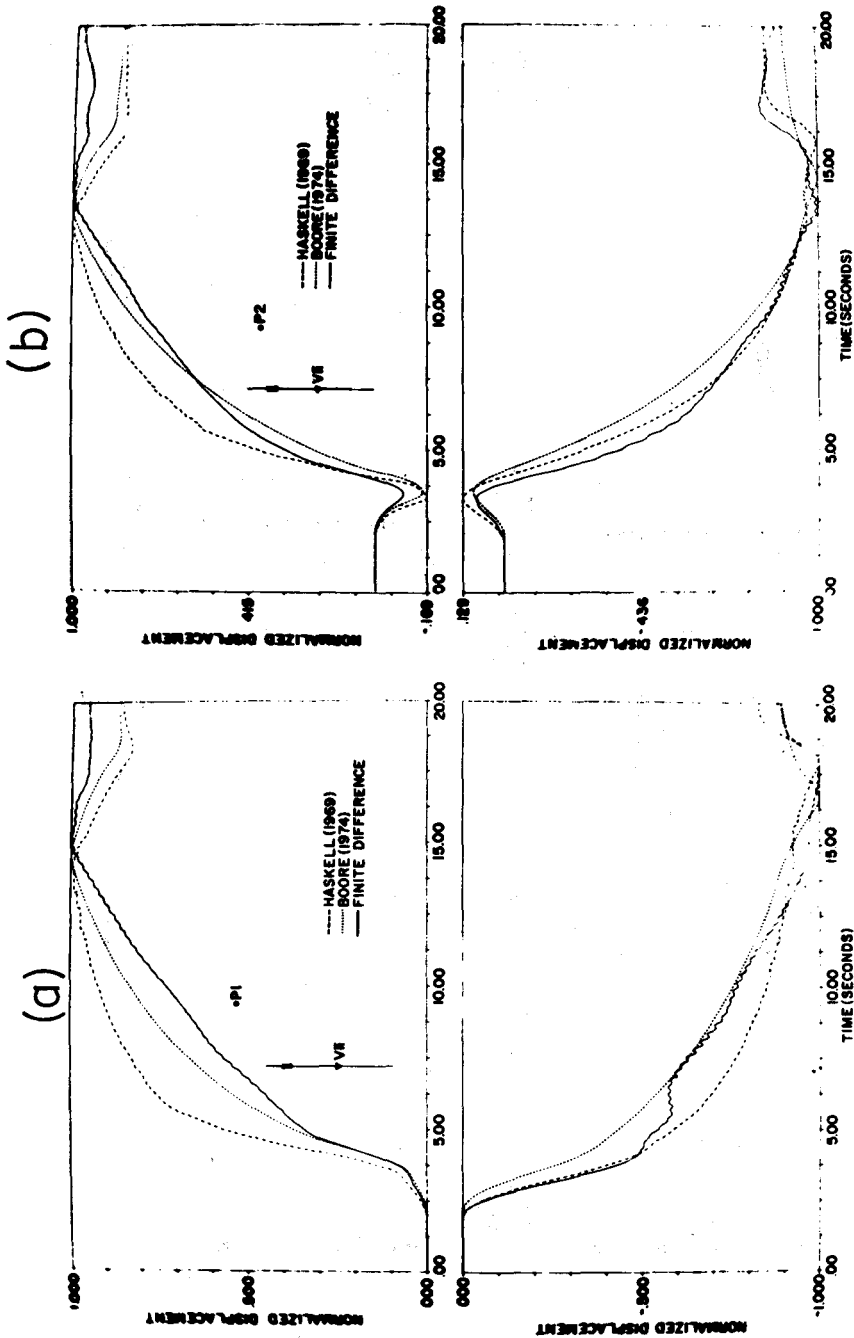
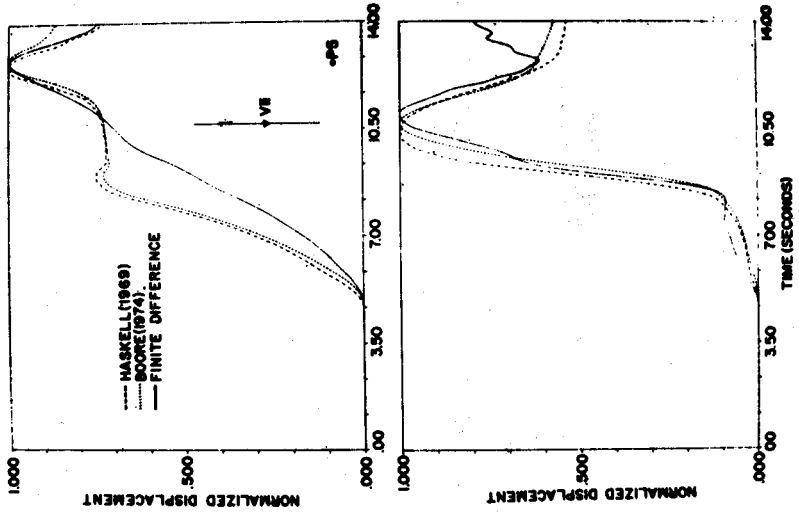
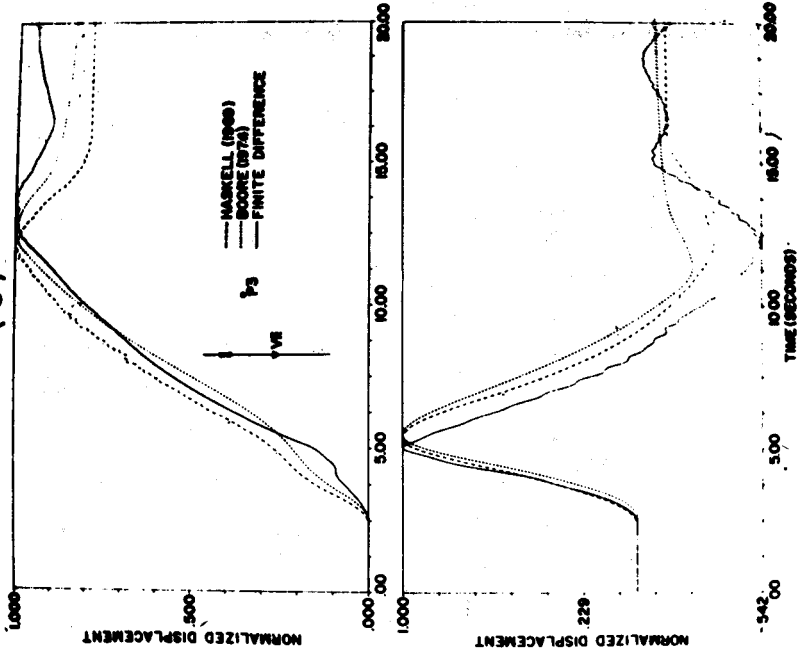


Fig. 4. Vertical and horizontal displacements at points (a)P1, (b)P2, (c)P3, (d)P4 and (e)P5. (---) Haskell (1969), (---) Boore and Zoback (1974), (---) finite-differences. The displacement is normalized to the maximum amplitude in the seismogram. The displacement at P5 is shown only to 14 sec. since the reflections in the F.D. model are much more pronounced, after this point.

(e)



(c)



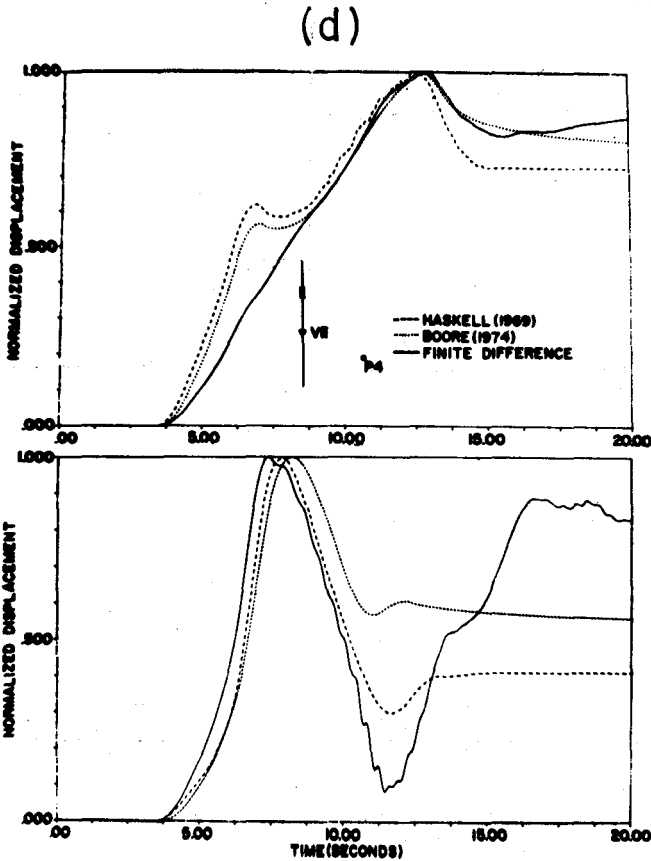


Figure 6 shows the case of a fault dipping  $60^\circ$  in a homogeneous medium. Synthetic seismograms will be shown of points  $S_1$  to  $S_{10}$ . The rupture starts at 0 and propagates upwards. A smooth time-history was used (shown at the top of Figure 6). All the other parameters are shown in the figure. Figure 7 displays the corresponding seismograms. It is readily noticed that the first arrival occurs in the seismograms of the right side first, as should be expected. Change of rupture velocity to 1 km/sec (Figure 8) produced a conspicuous broadening of the waveforms.

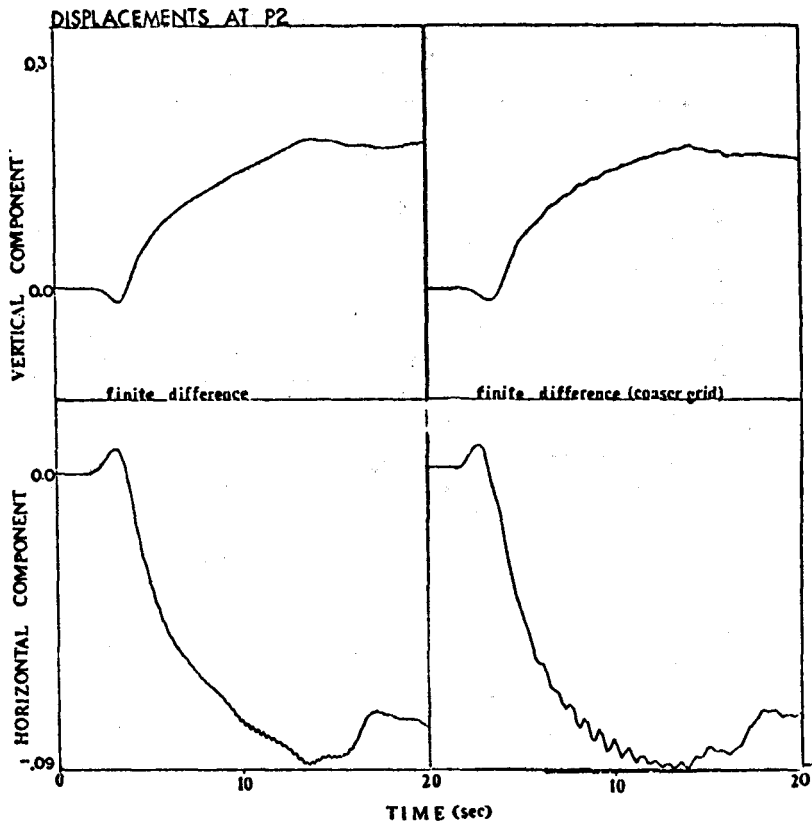


Fig. 5. Vertical and horizontal displacements at points P2 of the model of figure 3. The seismograms at left were obtained with a grid spacing of 0.6 and 0.2 sec time steps.

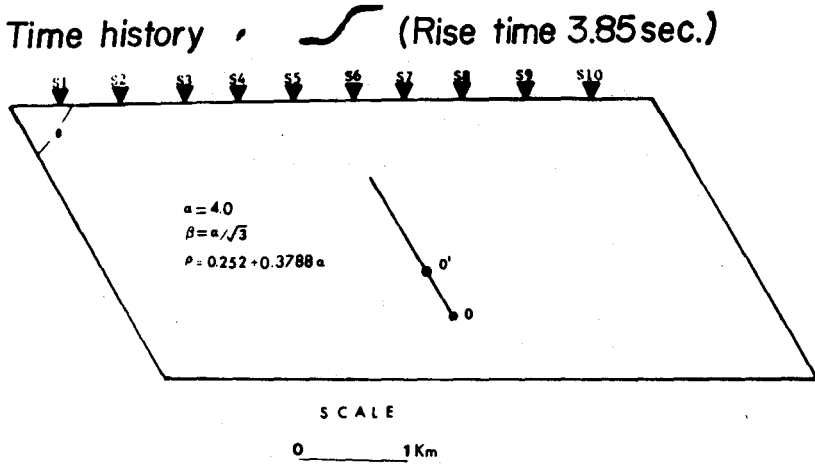


Fig. 6. Model employed to compute the seismograms of figures 7 to 10. The parameters are shown in the inserts. The model has 60 and 30 nodes in the horizontal and vertical directions respectively.

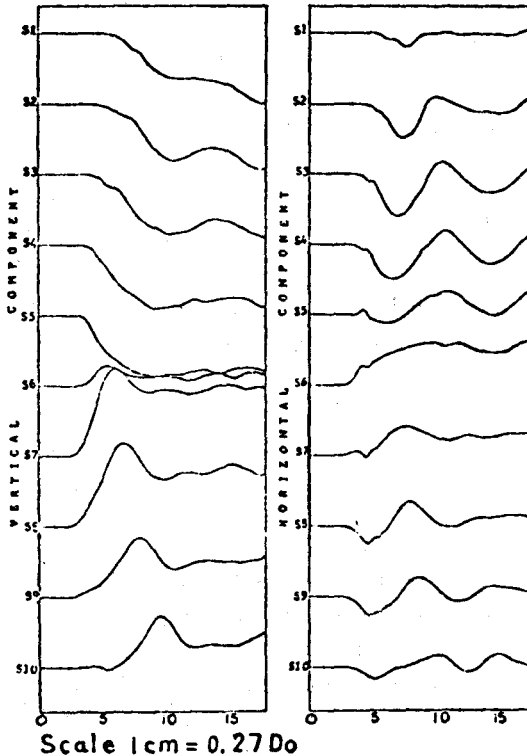


Fig. 7. Synthetic seismograms in the model of figure 6 and velocity of rupture ( $V_r$ ) of 2.0 km/sec. The slip is constant along the fault.

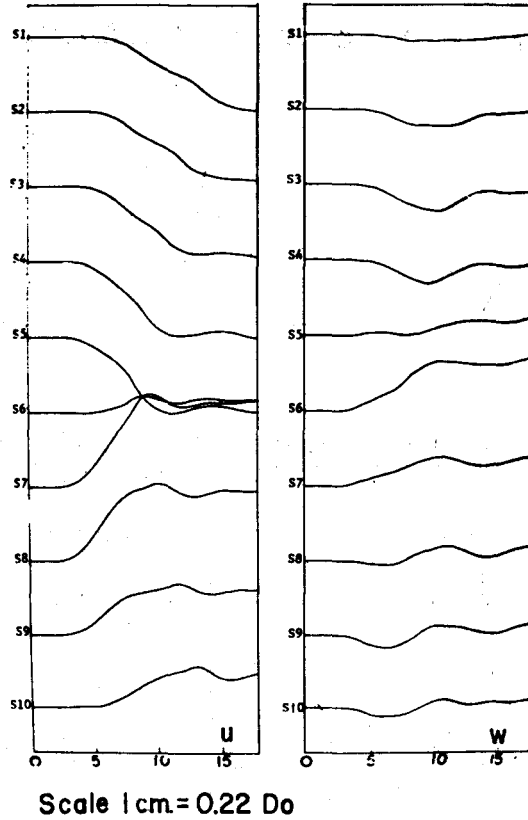
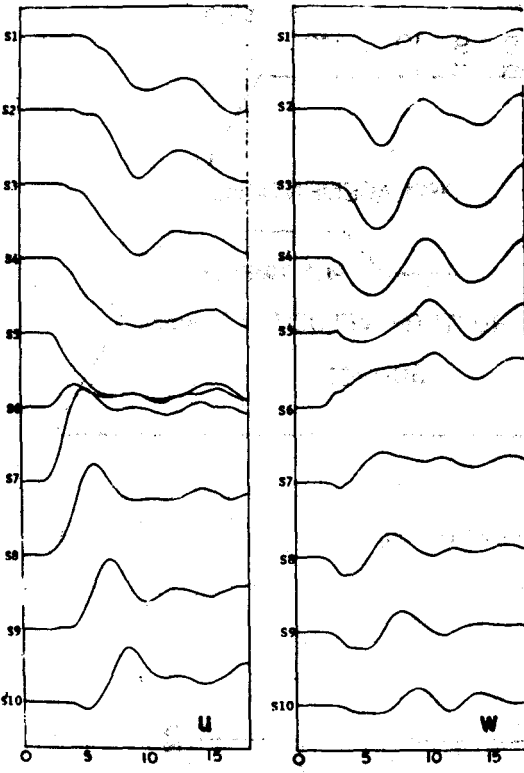
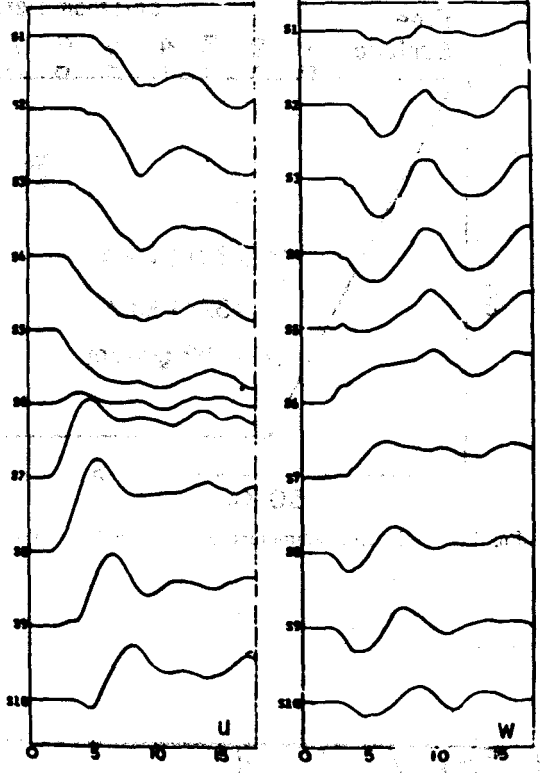


Fig. 8. As in figure 7 but with  $V_r = 1.0$  km/sec.

Assuming the same conditions as for the seismograms of Figure 7 but with bilateral constant faulting (starting at  $0^\circ$  in Figure 6) yields seismograms of different waveform but the amplitudes remain practically unchanged (Figure 9). If the slip across the fault is not constant but decreases smoothly toward the tips there is practically no change in the waveform (with respect to the bilateral constant case) but the amplitudes are decreased appreciably (Figure 10).



Scale 1 cm. = 0.27 Do



Scale 1 cm. = 0.08 Do

Fig. 9. As in figure 7 but with bilateral faulting of constant slip and  $V_r=2.0$  km/sec.

Fig. 10. As in figure 9. The slip is not constant but decays exponentially towards the tips.

The effect of the inhomogeneity of the medium will now be illustrated. In order to do this, consider first the situation of Figure 11. Here, we have a shallow reverse fault in a homogeneous half space. Figure 12 shows ground displacement at sites 1 to 10. The fault is practically a line source and the waveforms are simple to interpret. Some of the phases are shown on the first vertical component seismogram. With the same configuration and variables, except for the depth and length of the fault which is now 9.6 km long and 12 km deep, the seismograms of Figure 13 were generated. The waveforms are considerably different (apart from dispersion due to the use of the ramp function) and show the effects of this two factors. We turn now to the model of Figure 14 where all the variables are shown. The situation is similar

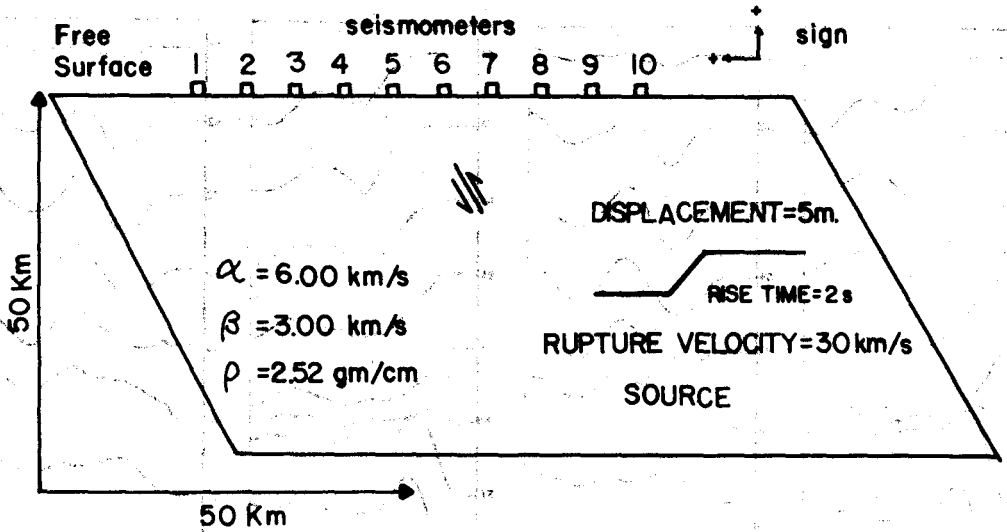
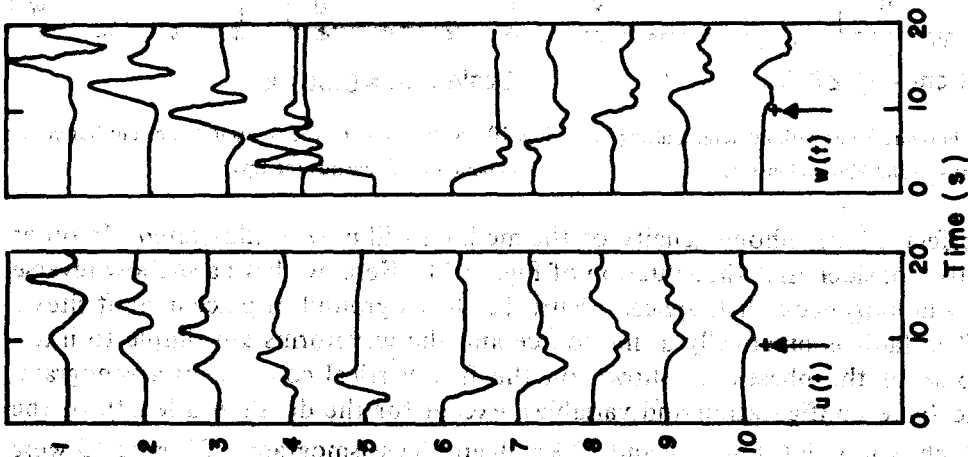


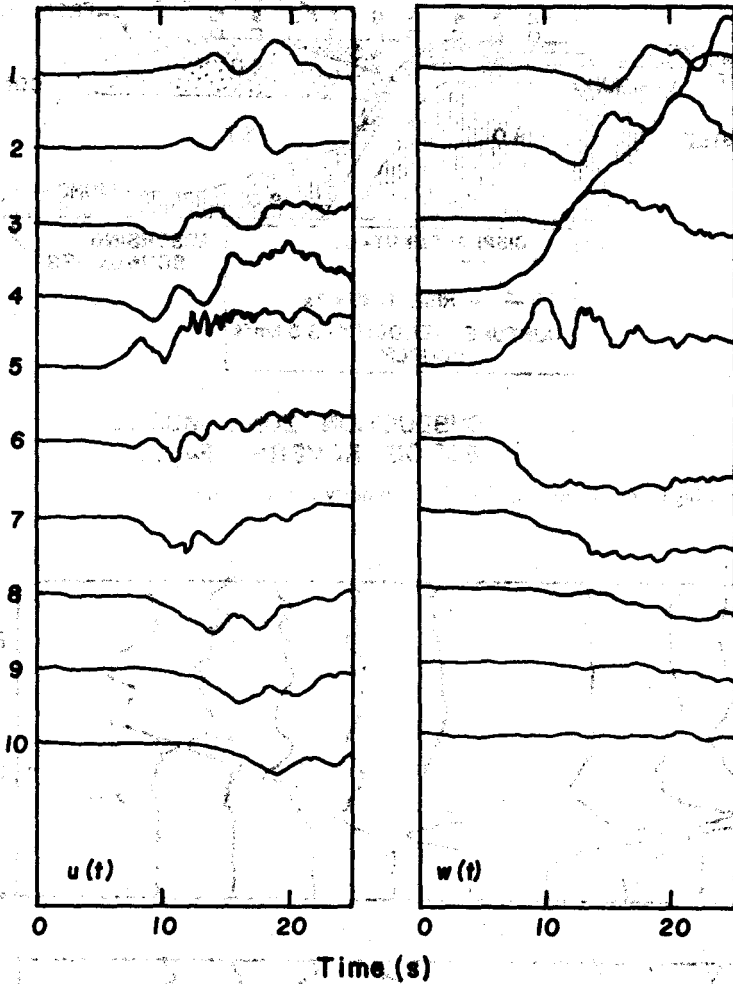
Fig. 11. Model and parameters to test the effect of the depth of the fault.



Scale 1 cm. = 0.04 Do

Fig. 12. Synthetic seismograms for the model of figure 11.

The fault is 4.4 km depth.



Scale 1 cm. = 0.01 Do

Fig. 13. As in figure 12 but with fault at 12 km depth and 9.6 km long.

to the above case except that the medium is not homogeneous. The velocity distribution is roughly for a subduction zone; of course no ocean is present in the model.

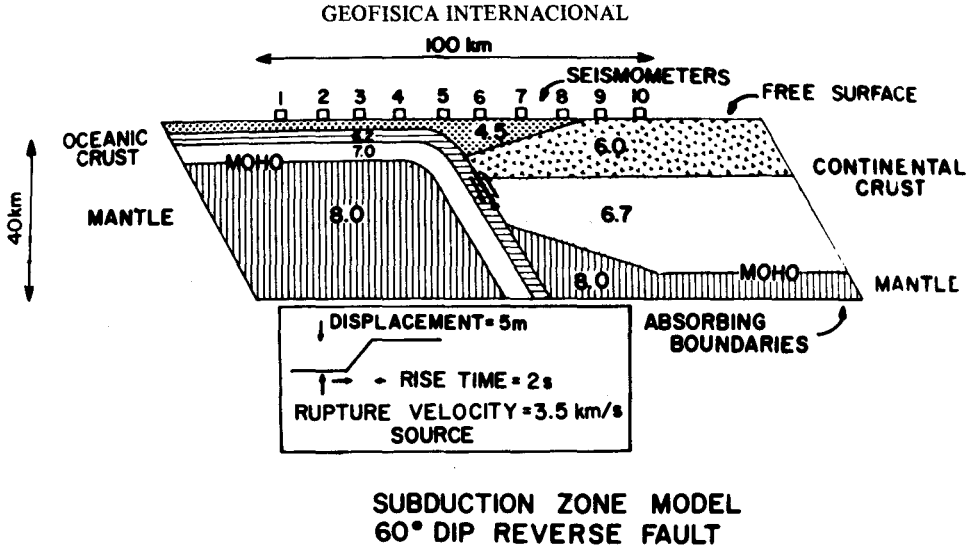


Fig. 14. Model showing heterogeneous media. The geometry is as in figure 11.

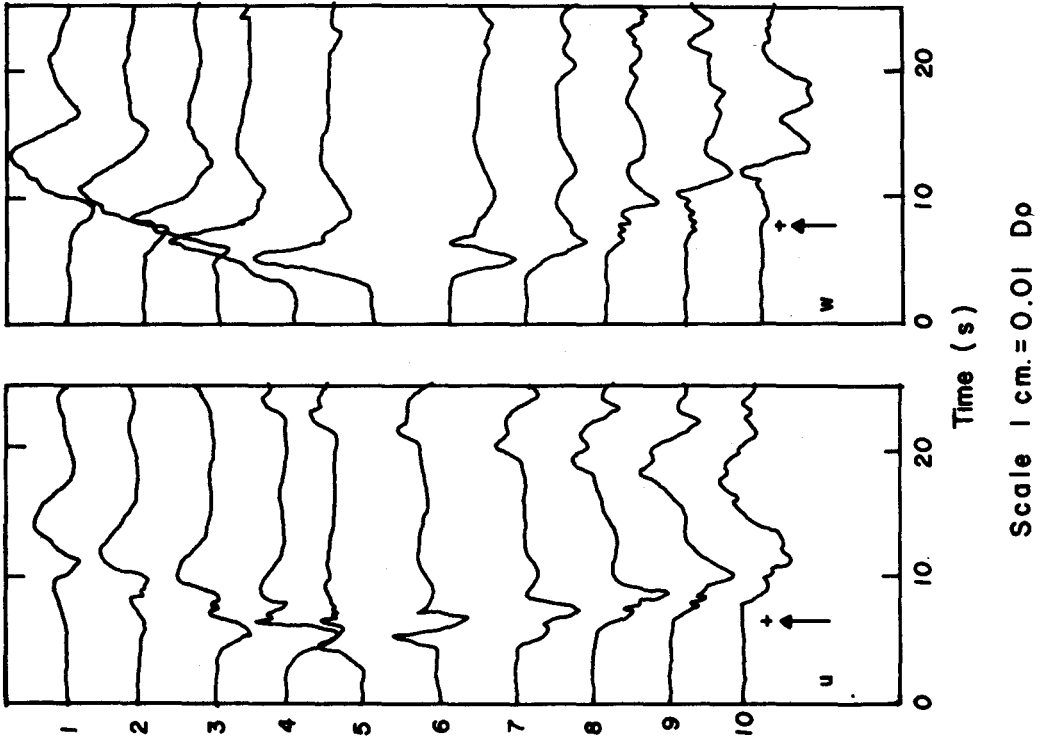


Fig. 15. Seismograms obtained for the model of figure 14. The fault is as in figure 13.

Figure 15 shows the corresponding seismograms. Their characteristics are completely different from those in Figure 13. Thus, not only the fault variables introduce changes in the waveforms (as between Figures 13 and 14) but the heterogeneity of the medium has a greater influence in the appearance of the waveforms.

### CONCLUSIONS

F-D techniques may be applied to the solution of the dislocation source problems with satisfactory results. Although some shortcomings are inherent to the method it provides solutions to a wide range of problems and it is therefore useful in modeling tectonic earthquakes or in the study of the effect of the various source parameters on ground motion.

### APPENDIX A

#### *The Wave Equation*

Equations (1) are easily changed to skew coordinates by means of the transformations (7); substitution of the differential operators by the approximations suggested by Kelly *et.al.* (1976) will yield the desired discrete approximations as follows.

For the two types of operators found, the approximations are:

$$\frac{\partial}{\partial x} \left[ \alpha^2(x, z) \frac{\partial u}{\partial x} \right] =$$

$$\frac{\alpha^2(m + 1/2, n) [u(m+1, n, \ell) - u(m, n, \ell)] - \alpha^2(m-1/2, n) [u(m, n, \ell) - u(m-1, n, \ell)]}{(\Delta h)^2}$$

where  $\alpha^2(m \pm 1/2, n) = \frac{\alpha^2(m \pm 1, n) + \alpha^2(m, n)}{2}$

and,

$$\frac{\partial}{\partial z} \left[ c^2(x, z) \frac{\partial}{\partial x} u(x, z, t) \right] =$$

$$\frac{\alpha^2(m, n+1) [u(m+1, n+1, \ell) - u(m-1, n+1, \ell)] - \alpha^2(m, n-1) [u(m+1, n-1, \ell) - u(m-1, n-1, \ell)]}{4\Delta h^2}$$

After substitution of this operator and solving for the displacement at time  $t+1$  we have:

$$\begin{aligned}
 u(m, n, \ell+1) = & 2u(m, n, \ell) - u(m, n, \ell-1) + \\
 & + F[ \alpha^2(m+1/2, n) (u(m+1, n, \ell) - u(m, n, \ell)) \\
 & - \alpha^2(m+1/2, n) (u(m, n, \ell) - u(m-1, n, \ell))] \\
 & + \frac{F}{4 \sin \theta} [ \alpha^2(m+1, n) (w(m+1, n+1, \ell) - w(m+1, n-1, \ell)) \\
 & - \alpha^2(m-1, n) (w(m-1, n+1, \ell) - w(m-1, n-1, \ell))] \\
 & - \frac{F}{\tan \theta} [ \alpha^2(m+1/2, n) (w(m+1, n, \ell) - w(m, n, \ell)) \\
 & - \alpha(m-1/2, n) (w(m, n, \ell) - w(m-1, n, \ell))] \\
 & - \frac{F}{2 \operatorname{sen} \theta} [ \beta^2(m+1, n) (w(m+1, n+1, \ell) - w(m+1, n-1, \ell)) \\
 & - \beta^2(m-1, n) (w(m-1, n+1, \ell) - w(m-1, n-1, \ell))] \\
 & + \frac{2F}{\tan \theta} [ \beta^2(m+1/2, n) (w(m+1, n, \ell) - w(m, n, \ell)) \\
 & - \beta^2(m-1/2, n) (w(m, n, \ell) - w(m-1, n, \ell))] \\
 & + \frac{F}{4 \operatorname{sen} \theta} [ \beta^2(m, n+1) (w(m+1, n+1, \ell) - w(m-1, n+1, \ell)) \\
 & - \beta^2(m, n-1) (w(m+1, n-1, \ell) - w(m-1, n-1, \ell))] \\
 & - \frac{F}{\tan \theta} [ \beta^2(m+1/2, n) (w(m+1, n, \ell) - w(m, n, \ell)) \\
 & - \beta^2(m-1/2, n) (w(m, n, \ell) - w(m-1, n, \ell))] \\
 & + \frac{F}{4 \sin \theta} [ \beta^2(m, n+1) (w(m+1, n+1) - w(m-1, n+1))]
 \end{aligned}$$

$$\begin{aligned}
 & - \beta^2(m, n-1) (w(m+1, n-1, \ell) - w(m-1, n-1, \ell)) \\
 & + \frac{F}{\sin^2 \theta} [ \beta^2(m, n+1/2) (u(m, n+1, \ell) - u(m, n, \ell)) \\
 & - \beta^2(m, n-1/2) (u(m, n, \ell) - u(m, n-1, \ell))] \\
 & - \frac{F \cos \theta}{4 \sin^2 \theta} [ \beta^2(m, n+1) (u(m+1, n+1, \ell) - u(m-1, n+1, \ell)) \\
 & - \beta^2(m, n-1) (u(m+1, n-1, \ell) - u(m-1, n-1, \ell))] \\
 & + \frac{F}{\tan^2 \theta} [ \beta^2(m+1/2, n) (u(m+1, n, \ell) - u(m, n, \ell)) \\
 & - \beta^2(m-1/2, n) (u(m, n, \ell) - u(m-1, n, \ell))] \\
 & - \frac{F \cos \theta}{4 \sin^2 \theta} [ \beta^2(m+1, n) (u(m+1, n+1, \ell) - u(m+1, n-1, \ell)) \\
 & - \beta^2(m-1, n) (u(m-1, n+1, \ell) - u(m-1, n-1, \ell))]
 \end{aligned}$$

Where  $F = \Delta t^2 / \Delta h^2$ .

After similar manipulations the vertical component is:

$$\begin{aligned}
 w(m, n, \ell+1) & = 2w(m, n, \ell) - w(m, n, \ell-1) \\
 & + \frac{F}{\sin^2 \theta} [ \alpha^2(m, n+1/2) [ w(m, n+1, \ell) - w(m, n, \ell) \\
 & - \alpha^2(m, n-1/2) w(m, n, \ell) - w(m, n-1, \ell) ] \\
 & - \frac{F}{4 \tan^2 \theta} [ \alpha^2(m, n+1) (w(m+1, n+1, \ell) - w(m-1, n+1, \ell)) \\
 & - \alpha^2(m, n-1) (w(m+1, n-1, \ell) - w(m-1, n-1, \ell))] \\
 & - \frac{F \cos \theta}{4 \sin^2 \theta} [ \alpha^2(m+1, n) (w(m+1, n+1, \ell) - w(m+1, n-1, \ell)) \\
 & - \alpha^2(m-1, n) (w(m-1, n+1, \ell) - w(m-1, n-1, \ell))]
 \end{aligned}$$

$$\begin{aligned}
& + \frac{F}{\tan^2 \theta} [\alpha^2(m+1/2, n)(w(m+1, n, \ell) - w(m, n, \ell)) \\
& - \alpha^2(m-1/2, n)(w(m, n, \ell) - w(m-1, n, \ell))] \\
& + \frac{F}{4 \sin \theta} [\alpha^2(m, n+1)(u(m+1, n+1, \ell) - u(m-1, n+1, \ell)) \\
& - \alpha^2(m, n-1)(u(m+1, n-1, \ell) - u(m-1, n-1, \ell))] \\
& - \frac{F}{2 \sin \theta} [\beta^2(m, n+1)u(m+1, n+1, \ell) - u(m-1, n+1, \ell)] \\
& - \beta^2(m, n-1)(u(m+1, n-1, \ell) - u(m-1, n-1, \ell))] \\
& + \frac{2F}{\tan \theta} [\beta^2(m+1/2, n)(u(m+1, n, \ell) - u(m, n, \ell)) \\
& - \beta^2(m-1/2, n)(u(m, n, \ell) - u(m-1, n, \ell))] \\
& + F[\beta(m+1/2, n)(w(m+1, n, \ell) - w(m, n, \ell)) \\
& - \beta^2(m-1/2, n)(w(m, n, \ell) - w(m-1, n, \ell))] \\
& + \frac{F}{4 \sin \theta} [\beta^2(m+1, n)(u(m+1, n+1, \ell) - u(m+1, n-1, \ell)) \\
& - \beta^2(m-1, n)(u(m-1, n+1, \ell) - u(m-1, n-1, \ell))] \\
& - \frac{F}{\tan \theta} [\alpha^2(m+1/2, n)(u(m+1, n, \ell) - u(m, n, \ell)) \\
& - \alpha^2(m-1/2, n)(u(m, n, \ell) - u(m-1, n, \ell))] \\
& - \frac{F}{\tan \theta} [\beta^2(m+1/2, n)(u(m+1, n, \ell) - u(m, n, \ell)) \\
& - \beta^2(m-1/2, n)(u(m, n, \ell) - u(m-1, n, \ell))]
\end{aligned}$$

These equations for  $v$  and  $w$  are as the ones in Kelly *et al.* (1976) when  $\theta = 90^\circ$  (note that this paper contains some misprints).

The derivation of the equation of motion when the density is assumed to be given by Birch's law may be derived in a similar manner. When  $\theta = 90^\circ$ . In this last case the operators will be of the type:

$$\frac{\partial}{\partial x} [\alpha^2(x, z) \rho(x, z) \frac{\partial u}{\partial x}(x, z, t)]$$

and

$$\frac{\partial}{\partial z} [\alpha^2(x, z) \rho(x, z) \frac{\partial u}{\partial x}(x, z, t)]$$

where the product  $\alpha^2(x, z) \rho(x, z)$  may be taken as a single variable.

#### APPENDIX B

##### *The Absorbing Boundary Conditions*

Equations (4a) and (4b) are paraxial approximations to the wave equation for waves travelling downwards. For sides other than the bottom, and for the corners, these equations must be rotated and then transformed to the skew coordinate system.

##### *Corners*

Clayton and Engquist show, as an example, the rotation of equation (4a) by an angle of  $45^\circ$ . Since their equation contains some misprints the derivation is repeated here for a general angle of rotation  $R$ . Note that this angle is different from the angle  $\theta$  of the skew coordinate system.

To facilitate the derivation, the following notation will be employed:

$$\frac{\partial}{\partial x} = D_x; \quad \frac{\partial}{\partial z} = D_z$$

double subscripts indicate double differentiation.

The rotation given by the matrix

$$\begin{pmatrix} \cos R & -\sin R \\ \sin R & \cos R \end{pmatrix}$$

is applied to equation (4a). After matrix multiplication and use of the chain rule on the derivatives it yields:

$$(D_z \cos R + D_x \sin R) \begin{pmatrix} u \cos R - w \sin R \\ u \sin R - w \cos R \end{pmatrix} + D_t \begin{pmatrix} 1/\rho & 0 \\ 0 & 1/\alpha \end{pmatrix} \begin{pmatrix} u \cos R - w \sin R \\ u \sin R + w \cos R \end{pmatrix} = 0$$

The transformation to the new systems is now applied (*i.e.*, equations (6)).

$$\left( \frac{1}{\sin \theta} (D_z - D_x \cos \theta) \cos R + D_x \sin R \right) \begin{pmatrix} u \cos R - w \sin R \\ u \sin R - w \cos R \end{pmatrix} \\ + D_t \begin{pmatrix} 1/\beta & 0 \\ 0 & 1/\alpha \end{pmatrix} \begin{pmatrix} u \cos R - w \sin R \\ u \sin R + w \cos R \end{pmatrix} = 0$$

From this matrix equation we obtain the following system of equations:

$$\frac{1}{\sin \theta} (D_z U c^2 - D_z w s c - (D_x U c^2 - D_x w s c) \cos \theta) + D_x U s c - D_x w s^2$$

$$+ \beta^{-1} D_t U c - \beta^{-1} D_t w s = 0$$

(B1)

$$D_x U s^2 - D_x w s c + \alpha^{-1} D_t U s + \alpha^{-1} D_t w c = 0$$

where:

$$U = U(m, n, \ell) ; \quad w = w(m, n, \ell)$$

$$s = \sin R \quad ; \quad c = \cos R$$

In order to apply these equations to the points on the corner, one sided finite differences are employed. The direction of the approximation (forward or backward operator) varies according to the position of the corner. Thus, in the lower-hand corner backward differences are used; in the upper corner of the same side, forward in  $z$  and backward in  $x$  and similarly on the other corners so that the points to be used fall within the model. The derivative with respect to time is similarly taken one-sided.

The differences may be written in a unique manner, regardless of the direction, writing the sign outside the operator. Thus,

$$D_z U = \text{SGN} \frac{(U(m, n, \ell) - U(m, 1, n\ell))}{\Delta H}$$

where  $SGN = 1$  if the difference is taken backwards, and  $SGN = -1$  if it is taken forward.

After substitution of the appropriate differences, equations (B1) result in a system of two equations in two unknowns. The solution of the system yield expressions for the displacements at the corners in terms of known values. The algebraic manipulation is omitted here, the final results being:

$$\begin{aligned}
 u(m, n, \ell) &= K_1 \cdot u(m, nM, \ell) + K_2 \cdot u(mN, n, \ell) + K_3 \cdot u(m, n, \ell-1) \\
 &\quad - K_4 \cdot w(m, nN, \ell) - K_5 \cdot w(nN, N, \ell) - K_6 \cdot w(m, n, \ell-1) \\
 w(m, n, \ell) &= K'_1 \cdot u(m, nN, \ell) + K'_2 \cdot u(mN, n, \ell) + K'_3 \cdot u(m, n, \ell) \\
 &\quad + K'_4 \cdot w(m, nN, \ell) + K'_5 \cdot w(mN, n, \ell) + K'_6 \cdot w(m, n, \ell)
 \end{aligned}$$

where:

$$K_1 = \left( \frac{sc}{hB \sin\theta} + \frac{c}{hA \sin\theta} \right) \frac{SGN1}{Du}$$

$$K_2 = \frac{s^2(SGN2)}{hB} - \frac{sc \cos\theta (SGN2)}{hB \sin\theta} - \frac{c \cos\theta (SGN2)}{hA \sin\theta} + \frac{cs(SGN2)}{hA}$$

$$K_3 = \left( \frac{c}{\beta A \Delta t} + \frac{s}{\alpha B \Delta t} \right) \frac{1}{Du}$$

$$K_4 = \left( \frac{c^2(SGN1)}{hB \sin\theta} - \frac{sc(SGN1)}{hA \sin\theta} \right) \frac{SGN1}{Du}$$

$$K_5 = - \frac{sc \cos\theta (SGN2)}{hA \sin\theta} + \frac{c^2 \cos\theta (SGN2)}{hB \sin\alpha} + \frac{s^2(SGN2)}{hA} - \frac{sc(SGN2)}{hB}$$

$$K_6 = \left( \frac{c}{\alpha B \Delta t} - \frac{s}{\beta A \Delta t} \right) \frac{1}{Du}$$

$$K'_1 = \left( \frac{sc}{hD \sin\theta} - \frac{c^2}{hC \sin\theta} \right) \left( \frac{SGN1}{Dw} \right)$$

$$K'_2 = \left( \frac{s^2}{hD} - \frac{sc}{hC} + \frac{c^2 \cos \theta}{hD \sin \theta} - \frac{sc \sin \theta}{hC \cos \theta} \right) \frac{(SGN2)}{Dw}$$

$$K'_3 = \left( \frac{s}{\alpha D \Delta t} - \frac{c}{\beta C \Delta t} \right) \frac{1}{Dw}$$

$$K'_4 = \left( \frac{sc}{hC \sin \theta} + \frac{c^2}{hD \sin \theta} \right) \frac{SGN1}{Dw}$$

$$K'_5 = \left( \frac{sc}{hD} + \frac{s^2}{hC} - \frac{sc \cos \theta}{hC \sin \theta} - \frac{c^2 \cos \theta}{hD \sin \theta} \right) \frac{SGN2}{Dw}$$

$$K'_6 = \left( \frac{c}{\alpha D \Delta t} + \frac{s}{\beta C \Delta t} \right) \frac{1}{Dw}$$

$$Du = \left( \frac{c^2}{hA} + \frac{sc}{hB} \right) \frac{SGN1}{\sin \theta} - \left( \frac{c^2 \cos \theta}{hA \sin \theta} - \frac{sc}{hA} - \frac{s^2}{hB} + \frac{sc \cos \theta}{hB \sin \theta} \right) SGN2 + \\ + \frac{s}{\alpha B \Delta t} + \frac{c}{\beta A \Delta t}$$

$$Dw = \left( \frac{sc}{hC} + \frac{c^2}{hD} \right) \frac{SGN1}{\sin \theta} - \left( \frac{sc \cos \theta}{hC \sin \theta} - \frac{s}{hC} + \frac{c \cos \theta}{hD \sin \theta} - \frac{sc}{hD} \right) SGN2 + \\ + \frac{s}{\beta C \Delta t} + \frac{c}{\alpha D \Delta t}$$

$$A = \frac{sc}{h \sin \theta} SGN1 - \frac{sc \cos \theta}{h \sin \theta} SGN2 + \frac{s^2}{h} SGN2 + \frac{s}{\beta \Delta t}$$

$$B = \frac{c^2}{h \sin \theta} SGN1 - \frac{c^2 \cos \theta}{h \sin \theta} SGN2 + \frac{sc}{h} SGN2 + \frac{c}{\alpha \Delta t}$$

$$C = \frac{c^2}{h \sin \theta} SGN1 - \frac{c^2 \cos \theta}{h \sin \theta} SGN2 + \frac{cs}{h} SGN2 + \frac{c}{\beta \Delta t}$$

$$D = \frac{sc}{h \sin \theta} SGN1 - \frac{sc \sin \theta}{h \cos \theta} SGN2 + \frac{s^2}{h} SGN2 + \frac{s}{\alpha \Delta t}$$

Here,  $h = \Delta H$  and  $SGN1$  and  $SGN2$  take the following values:

Corner	SGN1	SGN2
Lower right-hand side	1	1
Lower left-hand side	1	- 1
Upper right-hand side	- 1	1
Upper left-hand side	- 1	- 1

*Sides*

The rotation of the second order paraxial approximation for a general angle of incidence is quite cumbersome. Therefore, following Clayton and Engquist's procedure, the equations are rotated by multiples of  $\pi/2$  so that the walls show maximum absorbence at angles of incidence of  $90^\circ$ . These authors give equations for the four sides in terms of finite difference operators; however their expressions also contain misprints and are rederived here.

Equation (4b) with the notation used here is written as:

$$D_{tz}U + C_1 D_{tt}U + C_2 D_{tx}U + C_3 D_{xx}U = 0$$

Rotation of this equation by an angle of  $n\pi/2$  requires the transformation:

$$\begin{pmatrix} u' \\ w' \end{pmatrix} = \begin{pmatrix} \cos^{n\pi/2} & -\sin^{n\pi/2} \\ \sin^{n\pi/2} & \cos^{n\pi/2} \end{pmatrix} \begin{pmatrix} u \\ w \end{pmatrix}$$

where  $n = 1, 2, 3$  for the right, top and left sides respectively. In addition, application of the chain rule shows that:

$$\frac{\partial}{\partial z} = \frac{\partial}{\partial z} \cos \frac{n\pi}{2} + \frac{\partial}{\partial x} \sin \frac{n\pi}{2}$$

$$\frac{\partial}{\partial x} = \frac{\partial}{\partial x} \cos \frac{n\pi}{2} - \frac{\partial}{\partial z} \sin \frac{n\pi}{2}$$

Substitution of these expressions and the rotation matrix results in the following formulas for the sides:

Bottom:  $D_{zt}U + C_1 D_{tt}U + C_2 D_{tx}U + C_3 D_{xx}U = 0$

Top:  $D_{zt}U - C_1 D_{tt}U + C_2 D_{tx}U - C_3 D_{xx}U = 0 \tag{B2}$

$$\text{Right: } D_{xt}U + C_1 D_{tt}U + C_2 D_{tz}U + C_3 D_{zz}U = 0$$

$$\text{Left: } D_{xt}U - C'_1 D_{tt}U + C'_2 D_{tz}U - C'_3 D_{zz}U = 0$$

where  $C_1$ ,  $C_2$  and  $C_3$  are as before (equation (4b)) and

$$C'_1 = \begin{pmatrix} 1/\alpha & 0 \\ 0 & 1/\beta \end{pmatrix}; \quad C'_2 = (\beta - \alpha) \begin{pmatrix} 0 & 1/\alpha \\ 1/\beta & 0 \end{pmatrix};$$

$$C'_3 = \frac{1}{2} \begin{pmatrix} \alpha - 2\beta & 0 \\ 0 & \beta - 2\alpha \end{pmatrix}$$

Transformation of equations (B2) to skew coordinates yields:

$$\frac{1}{\sin\theta} D_{zt}U - \frac{\cos\theta}{\sin\theta} D_{xt}U + C_1 D_{tt}U + C_2 D_{tx}U + C_3 D_{xx}U = 0$$

$$\frac{1}{\sin\theta} D_{zt}U - \frac{\cos\theta}{\sin\theta} D_{xt}U - C'_1 D_{tt}U + C'_2 D_{tz}U - C'_3 D_{xx}U = 0$$

$$D_{xt}U + C_1 D_{tt}U + C_2 \left( \frac{1}{\sin\theta} D_{tz} - \frac{\cos\theta}{\sin\theta} D_{tz} \right) U + C_3 \left( \frac{1}{\sin^2\theta} D_{zz} - \frac{2\cos\theta}{\sin\theta} D_{xz} + \frac{\cos\theta}{\sin\theta} D_{xx} \right) U = 0$$

$$D_{xt}U - C'_1 D_{tt}U + C'_2 \left( \frac{1}{\sin\theta} D_{zt} - \frac{\cos\theta}{\sin\theta} D_{zt} \right) U - C'_3 \left( \frac{1}{\sin^2\theta} D_{zz} - \frac{2\cos\theta}{\sin\theta} D_{xz} + \frac{\cos\theta}{\sin\theta} D_{xx} \right) U = 0$$

Note that in changing coordinates the same notation is used for the displacement but this should not lead to confusion since it is clear that  $U = \begin{pmatrix} U \\ W \end{pmatrix}$  refers to the skew coordinate system.

In order to maintain consistency with respect to the points used in the calculations, Clayton and Engquist substitute the derivatives by difference operators concurrently taking averages in the displacements. The same procedure was followed in this work.

The equations for the top and bottom differ from the original equations by a new term and the factor  $\sin^{-1}\theta$  in the first member of the equation; this represents no special difficulty. After substitution of the difference operators and solution for the displacements on the boundaries at time  $t+1$ , one obtains:

$$\begin{aligned}
 U(m, n, \ell+1) = & S_1 (u(m, n-1, \ell+1) + u(m, n, \ell-1)) \\
 & + S_2 (u(m, n, \ell) + u(m, n-1, \ell)) - \\
 & - S_3 (w(m+1, n, \ell) - w(m+1, n, \ell-1) - w(m-1, n, \ell) \\
 & + w(m-1, \ell, j-1) + w(m+1, n-1, \ell+1) - w(m+1, n-1, \ell)) \\
 & \pm S_4 (u(m+1, n, \ell-1) + u(m-1, n, \ell-1) + u(m+1, n-1, \ell+1) \\
 & + u(m-1, m-1, \ell+1)) \\
 & + S_5 (u(m+1, n, \ell) - u(m+1, n, \ell-1) - u(m-1, n, \ell) \\
 & + u(m-1, n, \ell-1) + u(m+1, n-1, \ell+1) - u(m+1, n-1, \ell) \\
 & - u(m-1, n-1, \ell)) + u(m, n-1, \ell-1))
 \end{aligned}$$

where  $n = N$  if the equation is applied at the bottom

$$\begin{aligned}
 S_1 = \frac{A - B - 2S_4}{A+B} ; S_2 = \frac{2B}{A+B} ; S_3 = \frac{(\beta-\alpha)}{4\beta\Delta H\Delta t} ; \\
 S_4 = \frac{(\beta-2\alpha)}{4\Delta H^2} ; S_5 = \frac{\cos\theta}{A+B} ; A = \frac{1}{2\Delta H\Delta t \sin\theta} ; \\
 B = \frac{1}{2\beta\Delta t^2}
 \end{aligned}$$

The expressions for  $w(m, n, \ell+1)$  may be obtained from the above by exchange of  $w$  for  $u$  and  $\alpha$  for  $\beta$  with exception of  $S_3$  for which only the denominator changes. The same is true if instead of the bottom the equation is applied to the top, in the last case, in addition, the sign in the fourth member should be positive and  $n = 1$ .

The left and right sides are different in that the seventh term requires one sided differences in the  $x$  direction. In addition, the fourth member is also a coupling term and requires differentiation with respect to time. If a centered difference equation is used for the time derivative, as in the other members, the coupling of  $u$  and  $w$  occurs also at time  $t+1$  and a system of two equations and two unknowns must be solved.

The procedure is straightforward but involves a great deal of algebraic manipulation, hence only the final results are presented here. These were obtained by employing the same operators and averages of Clayton and Engquist and the ones listed below for the extra terms:

$$D_{tx} U = D_t^0 D_x^+ U(m, n, \ell)$$

$$D_{xz} U = D_x^+ D_z^0 U(m, n, \ell)$$

$$D_{xx} U = D_x^+ D_x^+ (U(m, n, \ell) + U(m+1, n, \ell))$$

The first term is multiplied by  $C_2$  which introduces the coupling.

The final formulas for the displacement are:

$$\begin{aligned} u(m, n, \ell+1) = & \left[ CK_1 + \frac{(\beta-\alpha)\cot\alpha}{2\alpha\Delta t\Delta H Q} (CK_2 - (w(m+1, n, \ell+1) - w(m+1, n, \ell-1) \right. \\ & + w(m, n, \ell-1)) - \frac{(\beta-\alpha)\cot\alpha}{2\beta\Delta t\Delta H Q} (u(m+1, n, \ell+1) - u(m+1, n, \ell-1) \\ & \left. + u(m, n, \ell-1)) \right] / \left( 1 - \frac{(\beta-\alpha)^2}{4\alpha\beta\Delta t\Delta H} \right) \end{aligned}$$

$$w(m, n, \ell+1) = CK_2 - \frac{(\beta-\alpha)\cot\alpha}{2\beta\Delta t\Delta H Q} (u(m+1, n, \ell+1) - u(m+1, n, \ell-1))$$

$$+ u(m, n, \ell-1) - u(m, n, \ell+1))$$

$$Ck_1 = (T_1 - T_2 - ((T_3 + T_4) \text{SIGN}) - (T_5 \text{SIGN}) - T_6 - T_7 + T_8) / A + B + E$$

$$T_1 = (a - B + 2D)(u(m+1, n, \ell+1) + u(m, n, \ell-1)) + 2B(u(m, n, \ell)$$

$$+ u(m+1, n, \ell))$$

$$T_2 = D(u(m+1, n+1, \ell-1) + u(m+1, n+1, \ell+1) + u(m+1, n-1, \ell-1)$$

$$+ u(m+1, n-1, \ell+1))$$

$$T_3 = C(w(m, n+1, \ell) - w(m+1, n+1, \ell-1) - w(m, n+1, \ell) + w(m+1, n+1, \ell-1))$$

$$T_4 = C(w(m+1, n+1, \ell+1) - w(m+1, n+1, \ell) - w(m+1, n-1, \ell+1) + w(m+1, n-1, \ell))$$

$$T_5 = 2D \cos\theta(u(m+1, n+1, \ell) - u(m, n+1, \ell) - u(m+1, n-1, \ell) + u(m, n-1, \ell))$$

$$T_6 = E(u(m, n, \ell-1) - u(m+1, n, \ell-1) - u(m+1, n, \ell-1) + u(m+2, n, \ell-1))$$

$$T_7 = E(u(m+2, n, \ell+1) - u(m+1, n, \ell+1) - u(m+1, n, \ell+1))$$

$$T_{10} = - (A+B) u(m+1, n, \ell)$$

$$A = \frac{1}{2\Delta t \Delta H} ; \quad B = \frac{1}{2\Delta t^2 \beta} ; \quad C = \frac{(\beta - \alpha)}{4\Delta t \Delta H \alpha \sin\theta} ;$$

$$D = \frac{(\alpha - 2\beta)}{4\Delta H^2 \sin^2\theta} ; \quad E = D \cos^2\theta ; \quad Q = A + B + E$$

$Ck_2$  and  $Q'$  can be obtained from  $Ck_1$  and  $Q$  by interchanging  $u$  and  $w$ ; and  $\alpha$  and  $\beta$  (except where  $(\alpha-\beta)$  appears). In this equation with  $m=1$  the left side is computed; with  $m=M$  the right one. Moreover,  $SIGN=1$  for the left side and  $SIGN=-1$  for the right one.

#### ACKNOWLEDGMENTS

Thanks are due to G. Rodríguez R. for typing the manuscript, and Mauro Pérez S. for drafting.

#### BIBLIOGRAPHY

- AKI, K., 1968. Seismic displacements near a fault. *J. Geophys. Res.* 72, 5359-5376.
- ALTERMAN, Z. and F. C. KARAL, Jr., 1968. Propagation of elastic waves in layered media by finite difference methods. *Bull. Seism. Soc. Am.*, 58, 367-398.
- ALTERMAN, Z. and D. LOWENTHAL, 1970. Seismic waves in a quarter and three quarter plane. *Geophys. J.* 20, 101-126.
- ANDERSON, J. G. and P. G. RICHARDS, 1975. Comparison of strong ground motion from several dislocation models. *Geophys. J.* 42, 347-373.
- BIRCH, F., 1964. Density and composition of mantle and core. *J. Geophys. Res.* 69, 4377-4388.
- BOORE, D. M., 1972. Finite difference methods for seismic wave propagation in heterogeneous materials, in *Methods in Computational Physics*, V. II, ed. B. A. Bolt. Academic Press, New York.
- BOORE, D. M. and M. D. ZOBACK, 1974. Near field motions from kinematic models of propagating faults. *Bull. Seism. Soc. Am.* 64, 321-342.
- BRUNE, J. N., 1970. Tectonics stress and the spectra of seismic shear waves from earthquakes. *J. Geophys. Res.* 75, 4997-5009.
- CLAYTON, R. and B. ENGQUIST, 1977. Absorbing boundary conditions for acoustic and elastic wave equations. *Bull. Seism. Soc. Am.* 67, 1529-1540.
- HASKELL, N. A., 1969. Elastic displacements in the near field of a propagating fault. *Bull. Seism. Soc. Am.*, 59, 865-908.
- ILAN, A., A. UNGAR and Z. ALTERMAN, 1975. An improved representation of boundary conditions in finite difference schemes for seismological problems. *Geophys. J.*, 43, 727-745.
- KELLY, K. R., R. W. WARD, S. TREITEL and R. M. ALFORD, 1976. Synthetic seismograms: a finite difference approach. *Geophysics*, 41, 2-27.

- MADARIAGA, R., 1978. The dynamic field of Haskell's rectangular dislocation fault model. *Bull. Seism. Soc. Am.*, 68, 869-887.
- SALVADORI, M. G. and M. L. BARON, 1961. Numerical methods in Engineering. Prentice Hall, Inc., New Jersey.